SOURCES OF SCATTER IN FRACTURE TOUGHNESS VALUES AND IN FATIGUE-CRACK PROPAGATION-RATES

J.F. Knott*

Micromechanical models for the fracture toughness of structural steel at low temperatures involve the propagation of microcracks formed in the plastic zone ahead of a precrack. The paper describes some of the critical microstructural units in higher-strength structural steels and treats the scatter in fracture toughness arising from effects of stress gradient and distribution of units. Results on two-phase microstructures and bimodal toughness distributions are discussed and attention is paid to the role of monotonic brittle fracture modes in fatigue-crack propagation.

INTRODUCTION

There are two distinct kinds of scatter in measurements of resistance to fast fracture or sub-critical crack propagation. The first is the variation in monotonic fracture toughness or crack growth-rate, measured in testpieces containing single, long pre-cracks. This is attributable to the size and distribution of microstructural features, such as grains, precipitates or non-metallic inclusions, and to the probability that a particular feature is located close to the tip of the pre-crack. The second kind of scatter arises when a testpiece or component does not contain any deliberately-introduced pre-crack or stress-concentrator. The testpiece is "smooth", but the material may contain a distribution of defects which, in the absence of a single, large pre-crack, act as "pre-cracks". Even if the material's matrix toughness remains constant from point to point, the overall toughness depends on the size of the largest defect, combined with its orientation to the maximum tensile stress or strain, and on any interaction between adjacent defects. In a matrix of low toughness, even a small defect can produce a dramatic decrease in fracture stress, but in engineering alloys used as tension members in structures, monotonic fracture is seldom affected by small defects and their most important effect is on properties such as the fatigue endurance.

Many of the microstructural features are common to both "long-crack" and "smooth" testpiece behaviour, and it is often appropriate to model the "long-crack" toughness in terms of a distribution of "defects" in the process-zone ahead of the pre-crack tip. The present paper treats aspects of this type of modelling for monotonic fracture in pre-cracked testpieces to illustrate the features which produce scatter. These conclusions are then assumed implicitly to apply to the occurrence of monotonic fracture modes in fatigue-crack propagation.

*Dept. Metallurgy and Materials Science, University of Cambridge, Pembroke Street, Cambridge CB2 3QZ, U.K.

SOURCES OF SCATTER IN FRACTURE TOUGHNESS

Micromechanisms of monotonic fracture in precracked testpieces may be described as cracking processes or rupture processes. In the present paper, only cracking processes are considered. Microcracks are initiated by plastic deformation ahead of a notch or pre-crack and the catastrophic propagation of one or more of these microcracks is determined by a critical value of the maximum tensile stress, σ_{max}, in the plastic zone. In a notched bar, the variation of tensile stress with distance below the notch shows a broad maximum, peaking a little way behind the plastic/elastic interface. Close to general yield, the stress rises from $0.9\sigma_{max}$ to σ_{max} and falls again to $0.9\sigma_{max}$ over a distance of approx. two root radii (Griffiths and Owen (1)); at 0.67 general yield, this distance is approx. 1.7 root radii. In a precracked specimen in plane strain, see fig.1 (after Tracey (2)) the peak occurs at a distance of 1.9δ (where δ is the C.O.D.) ahead of the crack tip: this is a fraction $(\sigma_y/0.04E)$ of the (minimum) extent of the plastic zone, r_{IY} (σ_y is the yield stress; E is Young's modulus). For $\sigma_y = 500\ MNm^{-2}$, the distance is approx. $r_{IY}/16$. The variation of stress with distance is sharp, rising from $0.9\sigma_{max}$ to σ_{max} and falling to $0.9\sigma_{max}$ over a total distance of approx. $0.008(K/\sigma_y)^2$.

Results from notched bars indicate that microcracks propagate when σ_{max} attains a critical value, σ_F, which, in mild steel, is relatively independent of temperature. Models have been developed to relate the values of σ_F obtained to microstructural features such as carbide size, grain size, martensitic or bainitic packet size, grain-boundary carbide size and impurity distribution (Knott (3), Jokl et al. (4)). If the microstructural "units" are homogeneously distributed and small with respect to the root radius, the variation in σ_F, and hence in the ratio P_F/P_{GY} (fracture load/general yield load) should be small, because a large number of units will be located in the high-stress region (between $0.9\sigma_{max}$ and σ_{max}). Statistically, there will always be a "weakest link" (maximum-size microcrack) in this region.

The principle underlying the relationship between fracture toughness, K_{Ic} and critical fracture stress, σ_F, can be written in terms of linear elastic (LEFM) analysis, although detailed calculations must make use of power-law hardening or elastic/plastic finite-element analyses. In LEFM, the stress, $\sigma(r)$, at a distance r ahead of a precrack, is given by:

$$\sigma(r) = K\ (2\pi r)^{-\frac{1}{2}} \qquad \ldots\ 1)$$

On rearrangement and setting the local stress $\sigma(r)$ equal to σ_F, a critical value of K, K_{Ic}, may be deduced, but only if an appropriate "critical distance" r*, can be identified:

$$K_{Ic} = \sigma_{F(r^*)}\ (2\pi r^*)^{\frac{1}{2}} \qquad \ldots\ 2)$$

Detailed calculations for a ferrite/grain-boundary carbide microstructure have been made by Ritchie et al. (5). Curry and Knott (6) have developed a model for transgranular cleavage crack propagation in spheroidised carbide microstructures. Here, in a given small region ahead of the precrack, it was possible to calculate the product of two probabilities: firstly, that the region contained a carbide of given size ($C > C_o$) and, secondly, that the stress across that region was sufficient to propagate a microcrack of size C_o. This model gave good agreement with experimental K_{Ic} results, which showed rather small scatter.

The same general principle may be applied to microstructures in higher-strength structural steels, although different critical microstructural units and distributions are found. Some examples are as follows:

i) in quenched-and-tempered (QT) structural steels, such as HY80 or A533B, the critical unit is the martensite or bainite packet size, ranging between approx. 5μm and 20μm for conventional heat-treatments, but approaching 100μm in coarse-grained heat-affected-zones (HAZ). In tempered steels the recrystallised ferrite grain size appears to be the critical unit (Fig.2);

ii) in temper-embrittled QT forging steels, there are two distributions: one of grain-boundary carbide size, one of degree of grain-boundary impurity segregation. Both these are (different) functions of grain-boundary misorientations. The prior-austenite grain size is typically 40μm;

iii) in C-Mn weld metals, there are microstructural distributions of coarse, grain-boundary ferrite (approx. 50μm in size) and fine, intra-granular, acicular ferrite (fig.3). Cracks propagate more easily in grain-boundary ferrite, but the nucleation of microcracks then appears to become a problem, because carbides would tend to be larger in the acicular regions. Tweed and Knott (7) have recently demonstrated the role of non-metallic inclusions (deoxidation products) in microcrack nucleation, and these are distributed fairly uniformly, both in grain-boundary ferrite and in acicular ferrite;

iv) in controlled-rolled steels, partial recrystallisation can cause a wide variation in ferrite grain size. Shehata and Boyd (8) have shown that it is the distribution of the coarsest grains (approx. 30μm) rather than the average grain size (∿ 5μm) which controls cleavage fracture;

v) in ferrite-pearlite microstructures, the micro-cracks form preferentially in the pearlite colonies. The volume fraction and size of these are functions of carbon content and cooling-rate, but, in a 0.4%C steel, might be 10-50μm in size.

The size of a microstructural unit determines the value of σ_F and the distribution of units determines the (statistical) value of "critical distance", r*. The average size of a unit is now much larger than that of a spheroidal carbide (perhaps 40μm compared with 1μm) and it is of interest to consider whether or not this will lead to an increase in scatter, if the units are randomly distributed. In the measurement of σ_F, using notched bars with Charpy root-radius (0.25mm), fractured between 0.67 general yield and general yield, the broad maximum in σ_{max} spreads over a distance of 1.7-2.0 root radii i.e. 425-500μm. Given the fact that the high stress is maintained also over a region of approx. 1 root radius (250μm) in the orthogonal (tangential) direction, the stress maximum exists over a region containing approx. 11 x 6 microstructural units. In two dimensions, the probability that one of these units is both coarse and favourably oriented to the applied stress is high. In the thickness direction (parallel to the notch root), there will also be a distribution of units and an unknown factor is the extent to which this will affect the probability of finding a "critical" unit. An argument, due to Cottrell (9) and based on localised flow between adjacent microcracks suggests that only two-thirds of the fracture surface need be cracked for total catastrophic propagation to occur. On this basis, a crude estimate of the number of units sampled in each "significant" thickness interval would be 100 rather than 66. The general conclusion is that, if units are distributed randomly, sufficient are sampled for a "weakest link" always to be present, so that σ_F should show rather little scatter.

In a precracked testpiece, it is convenient to use typical figures to establish the effect of sampling. For cleavage fracture at low temperature in a QT structural steel, take $K_{Ic} = 50$ MNm$^{-3/2}$, $\sigma_y = 750$ MNm^{-2}, $\sigma_F = 2250$ MNm^{-2}. The required value of $\sigma_{11(max)}/\sigma_y$ at fracture is then 3. From fig.1, this corresponds to $X/(K/\sigma_y)^2 = 0.015$, i.e. to $X = r^* = 67\mu m$. A 40µm unit ranges from 47µm to 87µm, corresponding to values of $\sigma_{11(max)}/\sigma_y$ falling from 3.28 to 2.77, i.e. to approx. $\pm$ 10% of the mean value. Two factors emerge. The first is that, even if the coarsest unit is sampled, there will be a variation in K of up to $\pm$ 5% (because r^* is proportional to K^2) depending on the centring of that unit with respect to the stress distribution. The second is that there is a much lower probability of sampling a "weakest link" unit by a specified value of $\sigma_{11(max)}/\sigma_y$, even if the lateral $\sigma_{11(max)}$ distribution is taken into account.

Interesting effects on the scatter in K_{Ic} values have recently been observed in two-phase metallic alloy microstructures by Hagiwara and Knott (10). Here, the specimens were heat-treated to produce different volume fractions of upper bainite in bainite/martensite microstructures in HY80 steel. The K_{Ic} values were observed to fall between two limits, corresponding to "100% martensite" ($\sigma_F = 3125$ MNm^{-2}; observed cleavage facet size 10µm), which was 57 ± 5 MNm$^{-3/2}$ and "100% bainite" ($\sigma_F = 2800$ MNm^{-2}, facet size 38µm), which was 42 ± 5 MNm$^{-3/2}$. These figures demonstrate the superior toughness of the low-carbon martensite and hence the importance of sufficient hardenability in QT structural steel for use in thick sections. At 40% bainite, the scatter was increased; two individual values of K_{Ic} of 44.7 and 56.0 MNm$^{-3/2}$ being recorded. The limits to r^* were calculated as 62µm for martensite and 46µm for upper bainite. Examination of the fracture surfaces of the two specimens containing 40% bainite along a line approx. 50µm ahead of the fatigue crack tip indicated that the facets were predominantly "bainitic" ($\sim$ 38µm) for the lower toughness value (44.7 MNm$^{-3/2}$) but predominantly "martensitic" ($\sim$ 10µm) for the higher toughness value (56 MNm$^{-3/2}$).

In a lamellar, banded microstructure of two phases, a bimodal distribution of toughness values may be envisaged and, indeed, it may be possible to attribute the "bimodal" results of Wilshaw and Pratt (11) to this effect, because they studied a rolled low-carbon steel which contained alternate bands of ferrite and pearlite. The scale of the banding and the strain-rate sensitivity of the fracture toughness of the (statically) tougher phase are of importance in determining whether or not the fracture of a more brittle phase is significant in terms of causing total instability or whether it simply produces a "pop-in". Consider perfect load control and a 100% banded mixture of two-phases: one with a toughness of 45 MNm$^{-3/2}$; the other with a (static) toughness of 55 MNm$^{-3/2}$. For a bend testpiece, with $(a/W) \simeq 0.5$ the stress intensity is given simply by $K = (P/BW^{\frac{1}{2}})Y(a/W)$, where $Y(a/W)$ is the tabulated compliance function: for $(a/W) = 0.47$ $Y(a/W) = 9.66$. If a given load P_F corresponds to fracture of the brittle phase with $K = K_{Ic} = 45$ MNm$^{-3/2}$, the same value of P_F will continue to produce fracture when $K_{Ic} = 55$ MNm$^{-3/2}$, provided that $Y(a/W)$ is increased to (55/45) 9.66 = 11.8. This corresponds to $(a/W) = 0.532$, i.e. to an increase in (a/W) of 0.06. If W is 25mm, this corresponds to 1.5mm, which implies a coarse scale of banding. It is clear that, to obtain bimodal distributions for finer-scale banding, the fracture toughness of the tougher phase must decrease sharply with increase in strain-rate, so that a crack which is accelerating through the more brittle phase can continue to propagate. Orientation is also important: if the bands are normal to the direction of crack propagation, "high-low" results may be obtained: if parallel, the scatter should be of the same order as that for the individual phases. Charpy impact results on weld metals obtained by Newmann, et al. (12) demonstrated a marked bimodality in behaviour. On the basis of the above argument, any bimodality in K_{Ic} or critical C.O.D. values is more likely to be due to distributions of the fine-grained and coarse-grained regions in the weld deposit than to the grain-boundary ferrite/acicular ferrite distribution *per se* (Fig.3). Fig.4 shows a welded specimens of the type used by (7), with the positions of a crack tip 0.06(a/W) apart indicated by A and B. This specimen was designed so that the crack tip would always be located in constant microstructure, but it is clear that, in general, specimens of weld-deposits cut in this orientation could show large scatter because the criterion would sometimes be met and sometimes not. Current recommendations for extraction of C.O.D. testpieces orient the crack tip so that it samples the whole deposit, including the root, to try to reduce this scatter.

EFFECTS ON FATIGUE GROWTH-RATES

This section briefly considers the effect of isolated "bursts" of brittle monotonic fracture on the macroscopic fatigue-crack growth-rate as measured, for example, using a potential drop system. The sensitivity of a system of this type is such that a change in crack length of approx. 10μm in a 10mm thick specimen can be detected, so that, based on equivalent areas, a single facet approx. 100μm x 100μm should be sufficient to produce a detectable change. Work by Ritchie and Knott (13,14) and Beevers et al. (15) has demonstrated the effects of both intergranular and transgranular cleavage and has shown that, in the latter case, the area fraction of cleavage facets, A_c, increases, between $0.7K_{Ic}$ and K_{Ic}, in an approximately linear fashion with K_{max}, the maximum stress intensity in the fatigue cycle. Alternatively, the term $(1-A_c)$ may be written as proportional to $(K_{Ic} - K_{max})$. Suppose now, that unit area of surface is broken under fatigue loading. For an R-ratio $(R = K_{min}/K_{max})$ of zero, the fatigue-crack growth-rate, for the striation mode, is $(da/dN)_o$. At a higher R-ratio, let a number of brittle facets form "instantaneously" during the propagation, so that the area which has to be traversed by striations is reduced to $(1-A_c)$. Hence, $(da/dN)_R = (da/dN)_o (1-A_c)^{-1} \propto (da/dN)_o (K_{Ic} - K_{max})^{-1}$. This simple model may then be used to predict effects of mean stress on crack growth-rate. The principle of "sectioning" a fracture surface by fatigue, which enables relationships between A_c and K_{max} to be determined experimentally, may be used further to study the growth of isolated facets as a function of K_{max}. This is an essential step in assessing effects of changes in microstructural distributions on the macroscopic fracture toughness.

ACKNOWLEDGEMENTS

Thanks are due to Professor R.W.K. Honeycombe F.R.S. for provision of research facilities and to Mr J.H. Tweed for useful discussions and permission to use previously unpublished micrographs.

SYMBOLS USED

A_c - area fraction of cleavage facets
a - crack length
(da/dN) - crack growth increment per cycle (growth-rate)
B - testpiece thickness
C, C_o - carbide size
E - Young's modulus
K, K_{Ic} - stress intensity factor, fracture toughness
K_{max}, K_{min} - maximum (minimum) K-values in fatigue cycle
P, P_F, P_{GY} - load, fracture load, general yield load
R - ratio of K_{min}/K_{max}
r, r^* - distance from crack tip, critical distance
r_{IY} - minimum extent of plastic zone
W - testpiece width

X - distance into plastic zone (fig.1)
$x_1 x_2$ - Cartesian coordinates
Y - compliance function
ν - Poisson's ratio
σ, σ_F - stress, local fracture stress
σ_{max} - maximum stress in plastic zone
σ_Y - yield stress

REFERENCES

1. Griffiths, J.R. and Owen, D.R.J., 1971, Jnl. Mech. Phys. Solids, 19, 419.
2. Tracey, D.M., 1973, Ph.D Thesis, Brown University, Providence R.I.
3. Knott, J.F., 1981 "Fracture Mechanics in Design and Service", Roy. Soc. (London), 45.
4. Jokl, M.L., Kameda, J., McMahon, C.J. and Vitek, V., 1980, Met. Sci., 14, 375.
5. Ritchie, R.O., Knott, J.F., and Rice, J.R., 1973, Jnl. Mech. Phys. Solids, 21, 395.
6. Curry, D.A. and Knott, J.F., 1979, Met. Sci., 13, 341.
7. Tweed, J.H. and Knott, J.F., 1982, this Conf.
8. Shehata, M.T. and Boyd, J.D., 1982 "Advances in the Physical Metallurgy and Applications of Steels", to be published. (Metals Soc.).
9. Cottrell, A.H., 1963, Proc. Roy. Soc. A276, 1.
10. Hagiwara, Y., and Knott, J.F., 1981, Proc. 5th Intl. Cong. on Fracture, ed. D. Francois, Pergamon, 2, 707.
11. Wilshaw, T.R. and Pratt, P.L., 1965, Proc. 1st Intl. Conf. on Fracture, Sendai, 973.
12. Newmann, A., Benois, F.F. and Hibbert, K., 1968, Schweisstechnik (Berlin) 18, 385.
13. Ritchie, R.O., and Knott, J.F., 1973, Acta Met., 21, 639.
14. Ritchie, R.O. and Knott, J.F., 1974, Matls. Sci. and Eng. 14, 7.
15. Beevers, C.J., Cooke, R.J., Knott, J.F. and Ritchie, R.O., 1975, Met. Sci. 9, 119.

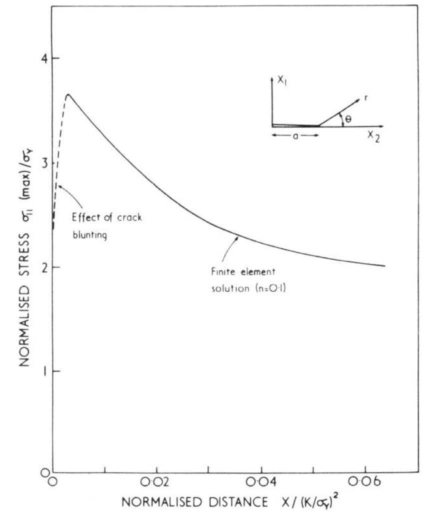

Figure 1 Distribution of Tensile Stress in Plastic Zone (after (2))

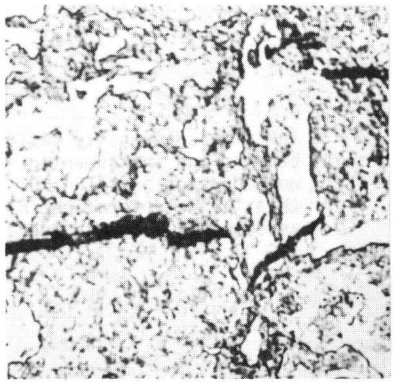

Figure 2 Microcracks in Tempered Alloy Steel x 1500

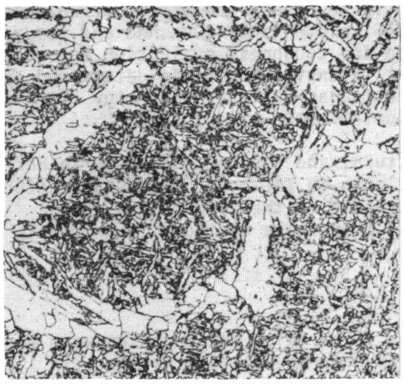

Figure 3 Grain-boundary Ferrite and Acicular Ferrite in C/Mn Weld Metal x 250 (courtesy J.H. Tweed)

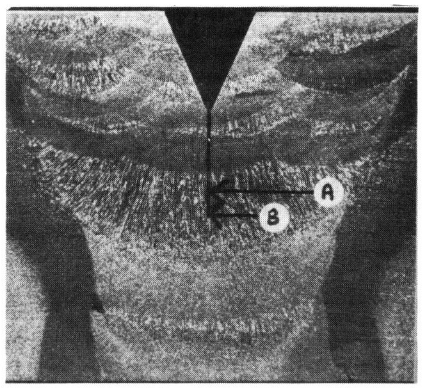

Figure 4 Weld-deposit, indicating (a/W) values varying by 0.06 x 7 (courtesy J.H. Tweed)